Identification and Functional Analysis of Tomato BRI1 and BAK1 Receptor Kinase Phosphorylation Sites[1][W][OPEN]

Vikramjit S. Bajwa[2], Xiaofeng Wang[3], R. Kevin Blackburn, Michael B. Goshe, Srijeet K. Mitra[4], Elisabeth L. Williams, Gerard J. Bishop, Sergei Krasnyanski, George Allen, Steven C. Huber, and Steven D. Clouse*

Department of Horticultural Science (V.S.B., X.W., S.K.M., S.K., G.A., S.D.C.) and Department of Molecular and Structural Biochemistry (R.K.B., M.B.G.), North Carolina State University, Raleigh, North Carolina 27695; Plant and Crop Sciences, University of Nottingham, Nottingham NG7 2RD, United Kingdom (E.L.W.); East Malling Research, East Malling, Kent ME19 6BJ, United Kingdom (G.J.B.); and United States Department of Agriculture/Agricultural Research Service, University of Illinois, Urbana, Illinois 61801 (S.C.H.)

Brassinosteroids (BRs) are plant hormones that are perceived at the cell surface by a membrane-bound receptor kinase, BRASSINOSTEROID INSENSITIVE1 (BRI1). BRI1 interacts with BRI1-ASSOCIATED RECEPTOR KINASE1 (BAK1) to initiate a signal transduction pathway in which autophosphorylation and transphosphorylation of BRI1 and BAK1, as well as phosphorylation of multiple downstream substrates, play critical roles. Detailed mechanisms of BR signaling have been examined in Arabidopsis (*Arabidopsis thaliana*), but the role of BRI1 and BAK1 phosphorylation in crop plants is unknown. As a foundation for understanding the mechanism of BR signaling in tomato (*Solanum lycopersicum*), we used liquid chromatography-tandem mass spectrometry to identify multiple in vitro phosphorylation sites of the tomato BRI1 and BAK1 cytoplasmic domains. Kinase assays showed that both tomato BRI1 and BAK1 are active in autophosphorylation as well as transphosphorylation of each other and specific peptide substrates with a defined sequence motif. Site-directed mutagenesis revealed that the highly conserved kinase domain activation loop residue threonine-1054 was essential for tomato BRI1 autophosphorylation and peptide substrate phosphorylation in vitro. Furthermore, analysis of transgenic lines expressing full-length tomato BRI1-Flag constructs in the weak tomato *bri1* allele, *curl3*^{abs1}, demonstrated that threonine-1054 is also essential for normal BRI1 signaling and tomato growth in planta. Finally, we cloned the tomato ortholog of TGF-β Receptor Interacting Protein (*TRIP1*), which was previously shown to be a BRI1-interacting protein and kinase domain substrate in Arabidopsis, and found that tomato TRIP1 is a substrate of both tomato BRI1 and BAK1 kinases in vitro.

Brassinosteroids (BRs) are regulators of plant growth and development that signal through the membrane-bound receptor kinase BRASSINOSTEROID INSENSTIVE1 (BRI1) and its coreceptor BRI1-ASSOCIATED RECEPTOR KINASE1 (BAK1; Li and Chory, 1997; Li et al., 2002; Nam and Li, 2002; Kim and Wang, 2010) to influence multiple physiological pathways involved in cell expansion and division, vascular differentiation, flowering, pollen development, and morphogenesis (Clouse, 2011b). Ligand-dependent phosphorylation of BRI1 and BAK1 modulates a cellular cascade of kinases and phosphatases (Kim et al., 2009; Tang et al., 2011) that ultimately results in the dephosphorylation and activation of two transcription factors, BRASSINAZOLE-RESISTANT1 (BZR1) and BRI1-EMS SUPPRESSOR1 (BES1; He et al., 2005; Yin et al., 2005), which in the presence of different interacting partners regulate the expression of over 1,000 genes associated with specific BR responses (Sun et al., 2010; Clouse, 2011a; Yu et al., 2011).

To better understand the mechanism of receptor kinase action in BR signaling, a series of studies using Arabidopsis (*Arabidopsis thaliana*) identified specific sites of serine (Ser), threonine (Thr), and tyrosine (Tyr) phosphorylation in both BRI1 and BAK1 that are critical for kinase function and effective BR signal transduction in planta, and models of the BRI1-BAK1 interaction and transphosphorylation were presented (Oh et al., 2000, 2009b, 2010; Wang et al., 2005, 2008). More than a dozen sites of phosphorylation have been identified in the BRI1 cytoplasmic domain, including the juxtamembrane domain, the catalytic kinase domain, and the

[1] This work was supported by the National Science Foundation (grant nos. MCB–0742411 and DBI–0619250), the U.S. Department of Agriculture Competitive Grants Program (grant no. NRI 2004–35304–14930), and the North Carolina Agricultural Research Service.

[2] Present address: Department of Plant Agriculture, University of Guelph, 50 Stone Road East, Guelph, Ontario, Canada N1G 2W1.

[3] Present address: Northwest A&F University, 3 Taicheng Road, Yang Ling, Shaanxi, China 712100.

[4] Present address: BASF, P.O Box 13528, Research Triangle Park, NC 27709.

* Address correspondence to steve_clouse@ncsu.edu.

The author responsible for distribution of materials integral to the findings presented in this article in accordance with the policy described in the Instructions for Authors (www.plantphysiol.org) is: Steven D. Clouse (steve_clouse@ncsu.edu).

[W] The online version of this article contains Web-only data.

[OPEN] Articles can be viewed online without a subscription.

www.plantphysiol.org/cgi/doi/10.1104/pp.113.221465

C-terminal region (Oh et al., 2000; Wang et al., 2005), and six or more sites have also been mapped in BAK1 (Wang et al., 2008; Karlova et al., 2009). Mutation of these essential regulatory sites to residues that are either nonphosphorylated or constitutively mimic phosphorylation can influence BRI1 and BAK1 kinase function and have dramatic effects on plant growth, development, and morphology. For example, mutation of the highly conserved BRI1 kinase domain activation loop residue Thr-1049 (and its corresponding residue Thr-455 in BAK1) to Ala results in complete loss of kinase activity in vitro and an extreme dwarf phenotype in vivo, suggesting that phosphorylation of this critical residue is required for BR signaling in planta (Wang et al., 2005, 2008). Phosphorylation of the BRI1 juxtamembrane residue Tyr-831 is not essential for kinase autophosphorylation in vitro but does confer regulatory properties in vivo, since the Y831F site-directed mutant has larger leaves and a higher photosynthetic rate than the wild type, suggesting that Tyr-831 is a negative regulatory site when phosphorylated (Oh et al., 2009a, 2011).

The identification of BR biosynthetic and insensitive mutants in tomato (*Solanum lycopersicum*; Bishop et al., 1999; Koka et al., 2000), rice (*Oryza sativa*; Yamamuro et al., 2000), barley (*Hordeum vulgare*; Chono et al., 2003), and pea (*Pisum sativum*; Nomura et al., 1997) clearly extended the importance of these compounds from the experimental plant Arabidopsis to crop plants. The Arabidopsis *bri1* mutant was initially isolated by a root growth inhibition screen for BR insensitivity (Clouse et al., 1996), and several independent genetic screens revealed over two dozen alleles of *bri1*, most of which exhibited the extreme dwarfism and other phenotypic characteristics of severe BR-deficient mutants (Kauschmann et al., 1996; Li and Chory, 1997; Noguchi et al., 1999; Friedrichsen et al., 2000). We previously identified a BR-insensitive mutant in tomato, *curl3* (*cu3*), that is phenotypically very similar to the Arabidopsis *bri1-1* mutant (Koka et al., 2000), and cloning the *CU3* gene from tomato showed that it encoded tomato BRI1 (SlBRI1), which also binds BR directly (Montoya et al., 2002; Holton et al., 2007). BRI1 homologs from several other crop species have also been cloned including rice, barley, and pea (Yamamuro et al., 2000; Chono et al., 2003; Nomura et al., 2003), and mutational analyses in both Arabidopsis and crop species have shown conclusively that the BRI1 receptor is required for normal BR perception and plant growth. However, a detailed analysis of BRI1 or BAK1 phosphorylation has not been reported in any plant other than Arabidopsis.

The cytoplasmic kinase domains of tomato and Arabidopsis BRI1 are highly conserved (82% identical), and many phosphorylated Ser, Thr, and Tyr residues previously identified in Arabidopsis BRI1 (Wang et al., 2005) occur in the same position in tomato SlBRI1, based on sequence alignment (Montoya et al., 2002). However, there are numerous residues in SlBRI1 that are not conserved in Arabidopsis BRI1 as well as conserved residues that are not phosphorylated in Arabidopsis, providing potential for differential BRI1 phosphorylation between the two species. Moreover, SlBRI1 did not rescue the weak *bri1-5* allele in Arabidopsis, indicating that BRI1 from the two species are not fully interchangeable (Holton et al., 2007). Differences between tomato and Arabidopsis in internal developmental cues, potential heterodimerization partners, and kinase domain substrates could yield differential patterns of BRI1 phosphorylation and gene expression between the two species. Thus, a detailed functional analysis of SlBRI1 phosphorylation sites and interacting proteins is required to determine the interspecies conservation and divergence of receptor kinase mechanisms involved in BR signaling. Here, we report the use of liquid chromatography-tandem mass spectrometry (LC-MS/MS) to identify in vitro sites of phosphorylation in SlBRI1 and SlBAK1 along with a functional characterization of a subset of these sites in kinase function and tomato growth and development.

RESULTS

SlBRI1-CD and SlBAK1-CD Have Autophosphorylation and Transphosphorylation Activities in Vitro

To determine if SlBRI1 and SlBAK1 are active kinases in vitro, the cytoplasmic domain of each Leu-rich repeat receptor-like kinase (LRR RLK) was cloned into *Escherichia coli* expression vectors conferring either an N-terminal Flag epitope tag or an N-terminal maltose-binding protein (MBP) tag to yield Flag-SlBRI1-CD, MBP-SlBRI1-CD, and MBP-SlBAK1-CD. The cloned cytoplasmic domains consist of the complete juxtamembrane region, kinase domain, and C-terminal region. The BRI1 constructs contain amino acids 824 to 1,207 of the previously published tomato BRI1 sequence (Montoya et al., 2002), while the cytoplasmic domain of MBP-SlBAK-CD shares 100% sequence identity with amino acids 254 to 617 of SlSERK3B, which has been shown by phylogenetic analysis to be the most likely tomato ortholog of Arabidopsis BAK1 (Mantelin et al., 2011). Putative kinase-inactive forms of tomato BRI1 (SlmBRI1-K916E) and BAK1 (SlmBAK1-K321E) were generated by mutating the conserved Lys residues in kinase subdomain II, which correspond to Arabidopsis BRI1 (K911E) and BAK1 (K317E) mutations, respectively, both of which lack kinase activity in vitro and in vivo (Wang et al., 2005, 2008).

Figure 1A shows that purified recombinant MBP-SlBRI1-CD, Flag-SlBRI1-CD, and MBP-SlBAK1-CD all exhibited substantial autophosphorylation activity when incubated under previously established assay conditions used for Arabidopsis BRI1 and BAK1 kinase analysis (Oh et al., 2000; Wang et al., 2005, 2008). Moreover, the mutated forms MBP-SlmBAK1-CD (K321E) and Flag-SlmBRI1-CD (K916E) showed no detectable kinase activity, as expected. When active Flag-SlBRI1-CD was incubated with kinase-inactive MBP-SlmBAK1, or when active MBP-SlBAK1-CD was incubated with

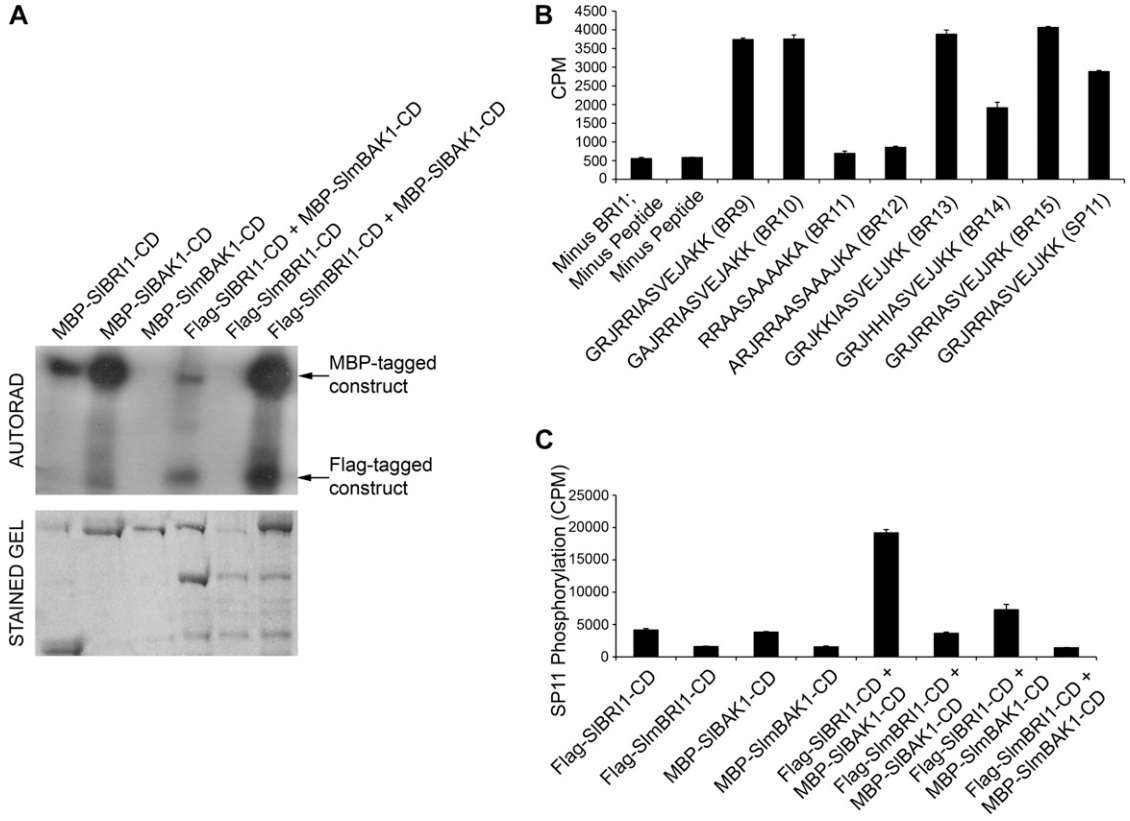

Figure 1. SlBRI1-CD and SlBAK1-CD are active kinases that can autophosphorylate and transphosphorylate in vitro. A, Autophosphorylation assays contained 1.0 μg of affinity-purified Flag-SlBRI1-CD, MBP-SlBRI1-CD, or MBP-SlBAK1-CD and 20 μCi of [γ-^{32}P]ATP in kinase buffer, followed by 10% (w/v) SDS-PAGE and autoradiography. B, Phosphorylation of synthetic peptides in vitro by 0.5 μg of Flag-SlBRI1-CD with 0.8 μCi of [γ-^{32}P]ATP and 0.10 mg mL^{-1} synthetic peptide in kinase buffer. J indicates nor-Leu, a nonoxidizing functional equivalent of Met. Error bars represent SE, and $n = 3$. C, Phosphorylation of the peptide substrate SP11 (GRJKKIASVEJJKK, where J = nor-Leu) by Flag-SlBRI1-CD (1.0 μg) is increased over 2-fold by the addition of MBP-SlBAK1-CD (1.0 μg) compared with the expected additive activity and is dependent on an active SlBAK1 kinase. Error bars represent SE, and $n = 3$.

kinase-inactive Flag-SlmBRI1-CD, both active kinases were able to transphosphorylate their kinase-inactive partners, similar to what has been previously shown for Arabidopsis BRI1 and BAK1 (Wang et al., 2008).

Recombinant Arabidopsis BRI1-CD phosphorylates synthetic peptides containing the previously determined consensus sequence for optimum BRI1 substrate phosphorylation, [RK]-[RK]-X(2)-[ST]-X(3)-[LMVIFY]-[RK], where one of the residues in brackets is the amino acid occurring at the indicated position and X represents any amino acid (Oh et al., 2000). To determine if SlBRI1-CD can recognize the same substrate sequences, peptide substrate phosphorylation assays were performed with Flag-SlBRI1-CD and a range of synthetic peptides previously characterized for Arabidopsis Flag-BRI1-CD (Oh et al., 2000). Flag-SlBRI1-CD phosphorylated synthetic peptides BR9, BR10, BR13, and BR15 at similar rates, while SP11 and BR14 supported reduced activity and BR11 and BR12 were both poor substrates (Fig. 1B). Overall, it appears that the sequence requirements for efficient substrate peptide phosphorylation by Flag-SlBRI1-CD are similar to those of Arabidopsis Flag-BRI1-CD, although some variations were evident. Flag-SlBRI1-CD phosphorylated BR9, BR10, BR13, and BR15 at higher levels than SP11 (Fig. 1B), while previous work in Arabidopsis showed that Flag-BRI1-CD relative velocity with respect to SP11 was greater than BR9, BR10, and BR15 and was exceeded only by BR13 (Oh et al., 2000). In fact, BR9, BR10, and BR15 had relative velocities at least 30% lower than BR13 in Arabidopsis, while all four were basically equally high in tomato. BR12 was a poor substrate for both tomato (Fig. 1B) and Arabidopsis Flag-BRI1-CD (Oh et al., 2000).

When the relative velocity of Flag-SlBRI1-CD against these SP11 variant peptides was compared (Fig. 1B), it was found that (1) changing the Lys at P+5, relative to the phosphorylated Ser ($P = 0$), in SP11 to an Arg (BR15) increases peptide phosphorylation by about 41%; (2) substituting Arg of SP11 at P$-$3 and P$-$4 with Lys (BR13) enhanced phosphorylation by about 35%, whereas replacement with His residues (BR14) decreased phosphorylation by approximately 34%; (3) substituting the

Arg residue at P−6 with Ala (BR10) increased peptide phosphorylation by 30%; (4) replacing the hydrophobic residue at P+4 of SP11 with Ala (BR9) also resulted in a 30% increase in phosphorylation; and (5) replacing Val, Glu, nor-Leu, Lys, and Gly at P+1, P+2, P+3, P+6, and P−7, respectively, of SP11 with Ala (BR12) reduced peptide phosphorylation by about 70%.

Transphosphorylation of Flag-SlBRI1-CD by MBP-SlBAK1-CD Increases BRI1 Kinase Activity in Peptide Substrate Phosphorylation Assays

Previous results in Arabidopsis have shown that BAK1 transphosphorylation of BRI1 on specific juxtamembrane and C-terminal domain residues enhances the ability of BRI1 to phosphorylate synthetic peptide substrates by at least 3-fold (Wang et al., 2008). To determine if the transphosphorylation between tomato BRI1 and BAK1 leads to increased kinase activity of either protein, MBP-SlBAK1-CD was incubated with Flag-SlBRI1-CD and their kinase activities were monitored by assessing phosphorylation levels of the synthetic peptide SP11. Flag-SlBRI1-CD alone phosphorylated the SP11 peptide to an equivalent extent as MBP-SlBAK1-CD alone (Fig. 1C), which is in contrast to Arabidopsis BAK1, which had no apparent direct activity on BRI1 substrate peptides (Wang et al., 2008). However, as was previously observed in Arabidopsis, the mixture of equal amounts of MBP-SlBAK1-CD and Flag-SlBRI1-CD increased the level of peptide substrate phosphorylation significantly (Fig. 1C). Compared with their additive activity, the mixture of equal amounts of MB-SlBAK1-CD and Flag-SlBRI1-CD increased the level of peptide phosphorylation more than 2-fold. This enhancement in phosphorylation was dependent on MBP-SlBAK1-CD kinase activity, because substitution of the kinase-inactive form, MBP-SlmBAK1-CD, resulted in greatly reduced SP11 phosphorylation by BRI1. The kinase-inactive forms Flag-SlmBRI1-CD and MBP-SlmBAK1 were also unable to phosphorylate the SP11 peptide either alone or in combination.

Kinetics of Flag-SlBRI1-CD on Peptide Substrate Phosphorylation in Vitro

To determine if Flag-SlBRI1-CD phosphorylated substrate peptides SP11 and BR13 with realistic kinetics comparable to other known peptide substrates of plant kinases, we calculated K_m and V_{max} for both peptides with Lineweaver-Burk analyses using reaction velocities measured with seven substrate concentrations (Fig. 2). The K_m values of BR13 (109 μM) and SP11 (193 μM) do indeed fall within the range of K_m values for plant kinases with synthetic peptide substrates that reflect true physiological substrates, such as the cauliflower (*Brassica oleracea*) HMR kinase with a K_m of 95 μM for the SAMS peptide (Weekes et al., 1993). Flag-SlBRI1-CD showed higher apparent affinity for BR13 than for SP11 (K_m of 109 versus 193 μM, respectively) but lower V_{max} for BR13 compared with SP11 (Fig. 2). The selectivity of Flag-SlBRI1-CD for the two substrates can be expressed as the V_{max}/K_m ratio when the amount of enzyme is constant and was nearly identical for BR13 and SP11 (4.35 versus 4.86, respectively). It was previously reported that Arabidopsis Flag-BRI1-CD also had a higher affinity for BR13 than for SP11 (K_m of 81.7 versus 427 μM, respectively), but the V_{max}/K_m ratio for BR13 was 2.5 times higher than for SP11 (Oh et al., 2000). Overall, these data indicate that tomato and Arabidopsis BRI1 proteins are similar but not identical in terms of peptide substrate phosphorylation in vitro.

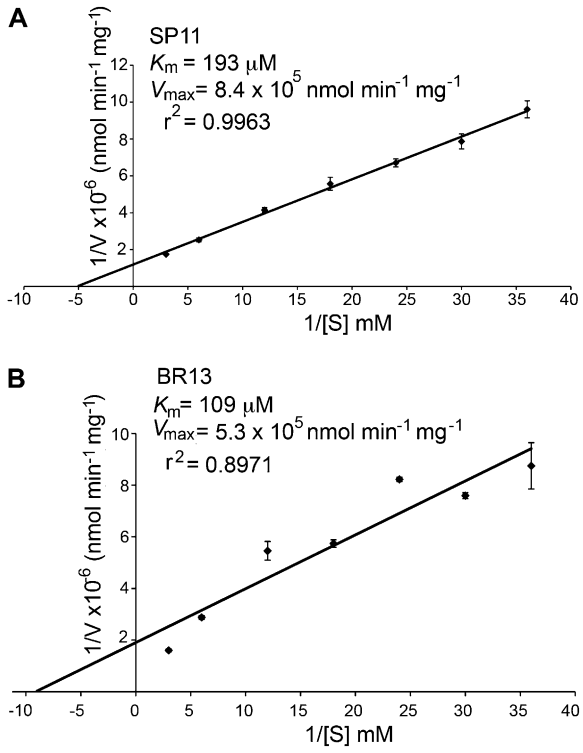

Figure 2. Peptide substrate kinetics of SlBRI1-CD. Lineweaver-Burk double reciprocal plots for SP11 (A) and BR13 (B) were constructed using the indicated substrate concentrations, 0.5 μg of Flag-SlBRI1-CD and 0.1 mM ATP (888 cpm pmol^{-1}), in kinase buffer. Error bars represent SE, and n = 3.

Tomato BRI1 Autophosphorylates on Multiple Ser, Thr, and Tyr Residues in Vitro

We previously identified at least 11 sites of in vivo phosphorylation in BRI1 by immunoprecipitation from BR-treated Arabidopsis seedlings followed by LC-MS/MS analysis and also found that Flag-BRI1-CD autophosphorylation sites identified in vitro were highly predictive of in vivo phosphorylation (Oh et al., 2000; Wang et al., 2005). To identify specific phospho (p)Ser, pThr, and pTyr phosphorylation sites in MBP-SlBRI1-CD, the autophosphorylated recombinant protein was subjected to SDS-PAGE, followed by gel extraction,

reduction, alkylation, and tryptic digestion. The digested peptides were extracted and subjected to quadrapole time-of-flight (Q-TOF) LC-MS/MS analysis, with or without immobilized metal affinity chromatography to enrich for phosphopeptides. The phosphorylated peptides identified are listed in Table I, and product ion spectra are shown in Supplemental Figure S1.

The sequence coverage of MBP-SlBRI1-CD was more than 85%, which resulted in five unambiguously assigned phosphorylation sites: Tyr-839, Thr-848, Ser-863 and Thr-877 in the juxtamembrane domain as well as Thr-1054 in the kinase domain activation loop (Table I). All of these juxtamembrane sites have been identified on the corresponding conserved Ser/Thr/Tyr residues in Arabidopsis BRI1 (Oh et al., 2000, 2009b; Wang et al., 2005). The highly conserved activation loop residue corresponding to tomato Thr-1054 (Thr-1049 in Arabidopsis BRI1) was shown by functional analysis to be critical for BRI1 kinase activity and signaling in Arabidopsis, and while likely phosphorylated, an unambiguous assignment of this site in Arabidopsis by LC-MS/MS analysis is not available (Oh et al., 2000; Wang et al., 2005). Our data provide tandem mass spectrometry spectral support that this residue is indeed phosphorylated in tomato. Moreover, based on manual inspection of product ion spectra, at least one and possibly up to three of the five sites (Thr-1040, Thr-1044, Ser-1047, Ser-1049, and Thr-1050) present in the activation loop of subdomain VII/VIII, spanning residues 1,032 to 1,061 of tomato BRI1, are likely to be phosphorylated (Table I). The length of the peptide, along with the presence of seven Thr and Ser residues in total, make unambiguous identification of the specific phosphorylation sites difficult. A similar situation occurred in the corresponding Arabidopsis activation loop peptide, where three of the six Ser/Thr residues were determined to be phosphorylated but their unambiguous location could not be determined (Oh et al., 2000; Wang et al., 2005).

Tomato BAK1 Autophosphorylates on Multiple Ser and Thr Residues in Vitro

Tryptic digested peptides from in vitro autophosphorylated MBP-SlBAK1-CD were subjected to Q-TOF LC-MS/MS (data dependent tandem mass spectrometry) or Q-TOF LC/MS^E (data independent mass spectrometry) analyses. The phosphorylated peptides identified are listed in Table I, and product ion spectra are shown in Supplemental Figure S2. Using these approaches, we identified tomato BAK1 phosphorylated residues Thr-290, Ser-294, Thr-453 and Thr-459, corresponding to Arabidopsis sites Ser-286, Ser-290, Thr-449, and Thr-455, which have been shown previously to be phosphorylated in vitro and in vivo (Wang et al., 2005, 2008). Phosphorylation at Arabidopsis

Table I. *SlBRI1, SlBAK1 and SlTRIP1 phosphorylation sites identified by Q-TOF LC-MS/MS or LC/MS^E*

Peptide[a]	Calculated M[b]	Measured M	Charge	Mascot Score[c]	PLGS Score[d]	Identified Site(s)	Correlating Arabidopsis Residue(s)
SlBRI1-CD in vitro sites							
EALpSINLAAFEKPLR	1,750.9018	1,750.8928	3	36	n/a[e]	Ser-863	Ser-858
EAALEAYMDGHSHSApTANSAWK	2,425.9998	2,425.9948	3	26	n/a	Thr-848	Thr-842
EAALEApYMDGHSHSApTANSAWK	2,505.9661	2,505.9568	3	21	n/a	Tyr-839, Thr-848	Tyr-831, Thr-842
KLpTFADLLEATNGFHNDSLVGSGGFGDVYK	3,251.5176	3,251.4901	4	28	n/a	Thr-877	Thr-872
LMSAMDTHLSVSTLAGpTPGYVPPEYYQSFR	3,397.5400	3,397.5490	3	20	n/a	Thr-1054	Thr-1049
LM*p(SAM*DTHLSVST)LAGTPGYVPPEYYQSFR[f]	3,429.5298	3,429.5374	3	17[g]	n/a	Ambiguous	Activation loop
SlBAK1-CD in vitro sites							
GpTIGHIAPEYLSTGK	1,622.7705	1,622.7724	2	40	10.29	Thr-459	Thr-455
GTIGHIAPEYLpSTGK	1,622.7705	1,622.7850	2	44	n.d.[h]	Ser-469	Thr-465[i]
ELQVApTDNFSNK	1,444.6235	1,444.6279	2	22	7.44	Thr-290	Ser-286
ELQVATDNFpSNKNILGR	1,997.9571	1,997.9617	2	28	7.78	Ser-294	Ser-290
pTQGGELQFQTEVEMISM*AVHR	2,486.0971	2,486.1022	3	n.d.[j]	6.84	Thr-328	Thr-324[i]
LLVYPYMANGp(SVAS)R[f]	1,719.8055	1,719.8178	2	n.d.[j]	6.9	Ser-374/Ser-377	Ser-370/Ser-373[i]
LM*DYKDTHVpTTAVR	1,744.7855	1,744.7680	3	50	7.12	Thr-453	Thr-449
LMDYKDp(THVTT)AVR[f]	1,728.7906	1,728.7750	3	39	8.24	Ambiguous	Thr-446/Thr-449/ Thr-450
SlBRI1-CD × mBAK1-CD transphosphorylation							
GpTIGHIAPEYLSTGK	1,622.7705	1,622.7772	2	34	n.d.[h]	Thr-459	Thr-455
SlBRI1-CD × SlTRIP1 transphosphorylation							
LAVIp(TT)DPFM*GLTSAIHIK[f]	2,123.0738	2,123.0361	3	45	n/a	Thr-111/Thr-112	Thr-111/Thr-112

[a]Met sulfoxide is denoted as M*; phosphoseryl, phosphotyrosyl, and phosphothreonyl residues are denoted as pS, pY, and pT, respectively. [b]M, Neutral monoisotopic mass. [c]Mascot scores are above the peptide identity threshold ($P < 0.05$) except as indicated. Spectra for all sites are provided in Supplemental Figures S1 (BRI1), S2 (BAK1), S3 (transphosphorylation), and S4 (TRIP1). [d]PLGS, ProteinLynx Global Server 2.4. [e]These data were analyzed by Mascot only. [f]At least one residue within the parentheses is phosphorylated, but the specific residue could not be assigned from spectral data. [g]This Mascot score was below the threshold level, but manual inspection of the spectrum confirmed phosphorylation of at least one of the residues within parentheses. See Supplemental Figure S1F for spectrum. [h]The PLGS search did not score this peptide. [i]Not previously reported as autophosphorylation sites in Arabidopsis BAK1. [j]The Mascot search did not score this peptide.

Thr-455, an activation loop residue equivalent to BRI1 Thr-1049, is essential for BAK1 kinase function and BR signaling in vivo (Wang et al., 2008). In addition to Thr-459, the activation loop residue Thr-453 (equivalent to Arabidopsis Thr-449) is phosphorylated in tomato BAK1, and two additional activation loop residues, Thr-450 and Thr-454 (equivalent to Arabidopsis Thr-446 and Thr-450) might also be phosphorylated but could not be unambiguously assigned based on available tandem mass spectrometry or data independent mass spectrometry product ion spectra. Furthermore, we also identified tomato BAK1 residues Thr-328, Ser-374 (or Ser-377), and Ser-469 as phosphorylation sites. The corresponding Arabidopsis residues Thr-324, Ser-370 (or Ser-373), and Thr-465 have not previously been reported as BAK1 phosphorylation sites.

Besides being autophosphorylated, the critical activation loop residue Thr-455 is also transphosphorylated by BRI1 in Arabidopsis (Wang et al., 2008). To determine if a similar BRI1/BAK1 transphosphorylation occurs in tomato, we incubated kinase-inactive MBP-SlmBAK1-CD with kinase-active Flag-SlBRI1-CD and found that, as in Arabidopsis, the tomato BAK1 activation loop residue Thr-459 was transphosphorylated by tomato BRI1 (Table I; Supplemental Fig. S3).

Effect of Mutating Identified and Predicted SlBRI1 Phosphorylation Sites on in Vitro Kinase Function

To understand the biochemical functions of the identified SlBRI1 phosphorylation sites, we used site-directed mutagenesis to generate 14 in vitro mutant constructs with selected Flag-SlBRI1-CD Ser, Thr, and Tyr residues substituted with Ala (for Ser and Thr residues) or Phe (for Tyr residues). The functional importance of each substituted residue was assessed by determining the effect on Flag-SlBRI1-CD autophosphorylation and on phosphorylation of the BR13 synthetic peptide. Mutating any of the S1040A, S1047A, and T1054A residues in the activation loop almost completely abolished kinase activity with respect to both autophosphorylation and peptide substrate phosphorylation (Fig. 3). The mutated activation loop residues T1044A and S1049A also showed dramatically reduced peptide substrate phosphorylation but did retain a residual amount of autophosphorylation activity. However, the T1050A activation loop mutation appeared to retain full activity in both assays.

Although the effects on kinase activity of mutating specific Ser/Thr residues in the activation loop of Flag-SlBRI1-CD were often similar to the effect of mutating

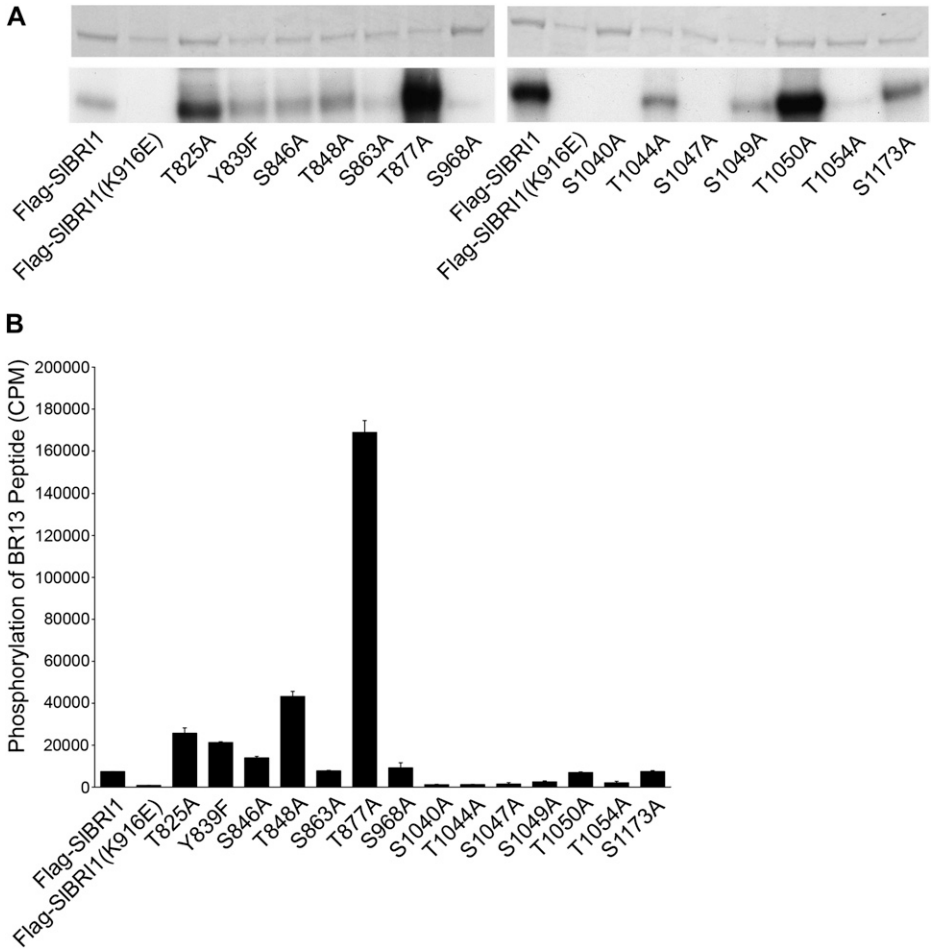

Figure 3. Effects of mutating specific Ser and Thr residues of Flag-SlBRI1-CD on in vitro autophosphorylation and substrate phosphorylation. A, Autoradiograph (bottom panel) showing autophosphorylation of recombinant Flag-SlBRI1-CD (the wild type) and a range of site-directed mutants. Loading of recombinant protein is shown by the stained gel in the top panel. B, Phosphorylation of a synthetic peptide (0.10 mg mL^{-1} BR13) with 0.5 μg of affinity-purified wild-type Flag-SlBRI1-CD or site-directed mutants. Error bars represent SE, and $n = 3$.

the corresponding residues in Arabidopsis Flag-BRI1, there were differences as well (Wang et al., 2005). Mutating the highly conserved residue Thr-1054 (equivalent to Arabidopsis Thr-1049) resulted in almost complete loss of kinase activity in both species. Similarly, tomato T1044A and the corresponding Arabidopsis T1039A both showed reduced peptide substrate phosphorylation but significant autophosphorylation activities. However, tomato S1047A showed no autophosphorylation activity, while the corresponding Arabidopsis residue S1042A showed substantial autophosphorylation (Wang et al., 2005). This suggests that Ser-1047 is critical for tomato BRI1 kinase function but the corresponding Arabidopsis Ser-1042 is not essential for BRI1 activity in that species.

With respect to juxtamembrane domain mutations, Y839F and T848A both retained autophosphorylation activity and both had significantly enhanced peptide substrate phosphorylation activity of 2.9- and 5.8-fold, respectively (Fig. 3). However, the corresponding Arabidopsis residues, Y831F (Oh et al., 2009b) and T842A (Wang et al., 2005), while retaining autophosphorylation activity, had reduced rather than enhanced phosphorylation of the BR13 peptide, suggesting different functions of these residues in the two species with respect to downstream substrate phosphorylation. However, tomato T877A had increased autophosphorylation and dramatically enhanced peptide substrate phosphorylation by more than 20-fold, similar to the corresponding Arabidopsis T872A mutation, which was previously shown to have enhanced BR13 phosphorylation of at least 10-fold (Wang et al., 2005).

In Vivo Functional Analysis of the SlBRI1 Thr-1054 Phosphorylation Site

The Arabidopsis *bri1-5* mutant is a weak allele that shows intermediate dwarfism and a smaller rosette size due to a C69Y amino acid substitution in the extracellular domain of BRI1 (Noguchi et al., 1999). Expression of wild-type Arabidopsis BRI1-Flag in the *bri1-5* mutant led to full rescue, while expression of BRI1-Flag with a T1049A substitution of the essential activation loop residue not only failed to rescue *bri1-5* but caused a dominant negative effect, with phenotypes similar to the extreme dwarfism of a *bri1-1* null allele (Wang et al., 2005). To understand the importance of the corresponding tomato BRI1 residue Thr-1054 in vivo, we generated transgenic tomato plants expressing wild-type *35S::SlBRI1-Flag* and *35S::SlBRI1-Flag* carrying the T1054A mutation, both in the $cu3^{-abs1}$ mutant background. The original *cu3* allele of tomato BRI1 is a null allele with an extreme dwarf phenotype, aberrant leaf structure, and male sterility (Koka et al., 2000), similar to Arabidopsis *bril-1* (Clouse et al., 1996), and like *bri1-1* in Arabidopsis, it is difficult to transform and propagate. However, $cu3^{-abs1}$ is analogous to Arabidopsis *bri1-5*, which as a weaker allele is clearly distinguishable from the wild type but is easier to transform and propagate than the null allele (Montoya et al., 2002). Phenotypic analysis of transgenic plants expressing wild-type SlBRI1-Flag in the $cu3^{-abs1}$ mutant demonstrated rescue of the dwarfism and curled, dark green, rugose leaf phenotype of the mutant plants (Fig. 4). However, SlBRI1-Flag(T1054A) failed to rescue the $cu3^{-abs1}$ mutant and, in fact, enhanced the dwarfism and altered leaf phenotype in a dominant negative effect with phenotypes similar to the *cu3* null allele (Fig. 4). Thus, as is the case for Arabidopsis Thr-1049, the BRI1 tomato activation loop residue Thr-1054 is essential for normal tomato growth and development.

SlBRI1-CD Phosphorylates Tomato TRIP1 in Vitro

We previously showed that Arabidopsis Flag-BRI1-CD could phosphorylate TGF-β Receptor Interacting Protein (TRIP1) in vitro on multiple Ser or Thr residues (Ehsan et al., 2005). To determine if Flag-SlBRI1-CD could also phosphorylate tomato TRIP1, a BLAST search of Arabidopsis TRIP1 (At2g46280) against the public tomato EST database was performed that resulted in the identification of an EST contig, TC195665, whose open reading frame shared 82% identity (91% similarity) to Arabidopsis TRIP1 across the entire 328-amino acid length of the TRIP1 protein. Conversely, a BLAST search of tomato unigene SGN-U575556 (the most recently updated and annotated version of TC195665, which corresponds to Solyc11g017070.1) showed 82% identity as expected with TRIP1 and only 30% identity with the next most closely related Arabidopsis sequence (transducin WD-40; At1g15470). Moreover, a BLAST search of SGN-U575556 against all nonredundant sequences in GenBank returned TRIP1 from many other

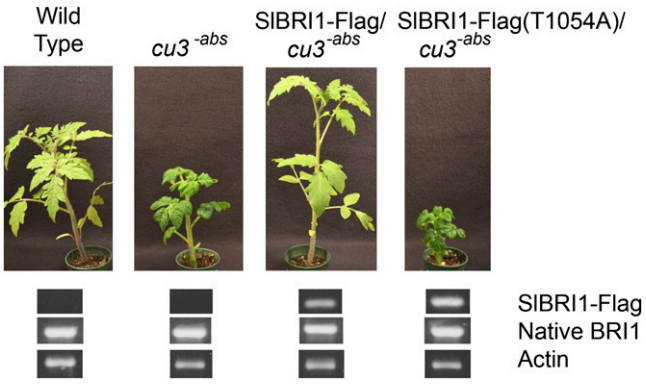

Figure 4. Effects of mutating the activation loop residue Thr-1054 of the SlBRI1 cytoplasmic domain on rescue of the SlBRI1 mutant, $cu3^{-abs1}$. Transgenic constructs 35S::SlBRI1-Flag and 35S::SlBRI1-Flag(T1054A) were transformed into the $cu3^{-abs1}$ background. All lines were grown together under the same greenhouse conditions and are the same age. Multiple independent lines for each construct were examined, and a typical plant with a representative phenotype for each line is shown. Expression levels of transgenes and native BRI1 were determined by PCR as described in "Materials and Methods."

plant species, as well as yeast (*Schizosaccharomyces pombe*), *Drosophila melanogaster*, and human, as the most closely related proteins. Since many of these TRIP1 proteins have a proven functional role as translation initiation factor eIF3i, it is highly likely that SGN-U575556 encodes the tomato ortholog of TRIP1/eIF3i. The full-length complementary DNA (cDNA) represented by SGN-U575556 was expressed in *E. coli* with an N-terminal Flag epitope tag, and the purified recombinant protein was incubated with either MBP-SlBRI1-CD or MBP-SlBAK1-CD. As shown in Figure 5, both kinases phosphorylated tomato TRIP1, although BRI1 appeared to have greater activity toward this substrate than BAK1. LC-MS/MS analysis identified either Thr-111 or Thr-112 (either residue was equally likely based on the acquired product ion spectra) as a SlBRI1-CD phosphorylation site of Flag-SlTRIP1 (Supplemental Fig. S4A). Thr-112 is a highly conserved residue and appears in Arabidopsis, tomato, bean (*Phaseolus vulgaris*), Drosophila, human, and yeast TRIP1 (Supplemental Fig. S4B).

DISCUSSION

The BR signal transduction pathway is one of the best understood in plants (Kim and Wang, 2010; Wang et al., 2012). However, most of our mechanistic understanding is based on research done in the model plant Arabidopsis, and significantly less detail regarding BR signaling has been revealed in crop plants. Field experiments have shown that slight modulations in rice BRI1 expression can alter rice yields by up to 30% (Morinaka et al., 2006), suggesting that understanding the molecular mechanism of BR signal transduction in tomato may also have practical implications in generating plants with valuable agronomic traits, such as altered growth architecture, enhanced photosynthesis, and increased yields. Numerous studies have confirmed the importance of BRI1 and BAK1 phosphorylation in regulating BR signal transduction in Arabidopsis. Brassinolide binding to the extracellular domain of BRI1 (Hothorn et al., 2011; She et al., 2011) results in activation of the BRI1 intracellular kinase domain and subsequent transphosphorylation and activation of BAK1, followed by reciprocal BAK1 transphosphorylation of BRI1, which enhances its kinase activity toward specific substrates (Wang et al., 2005, 2008). In order to compare the mechanisms of the early events in BR signaling between Arabidopsis and tomato, it is essential to identify and functionally characterize tomato BRI1 and BAK1 phosphorylation sites.

As expected, based on previous work with Arabidopsis BRI1 and BAK1, the recombinant Flag-SlBRI1-CD and SlBAK1-CD proteins had kinase activity in vitro, as evidenced by both autophosphorylation and also transphosphorylation of each other as well as of synthetic peptide substrates. The site-directed mutants Flag-SlmBRI1-CD (K916E) and MBP-SlmBAK1-CD (K321E), where the conserved Lys residue of subdomain II is substituted with Glu, produced inactive kinases, indicating that the activity observed with the native sequence proteins was the result of the tomato kinases and not a contaminating bacterial kinase. In order to identify the structural elements required for optimal substrate phosphorylation by Arabidopsis BRI1, peptide substrates having specific variation in their sequence were previously used for in vitro kinase assays (Oh et al., 2000). The optimal peptide sequences thus identified were further used to test the in vitro functional importance of BRI1 autophosphorylation sites (Wang et al., 2005) and also to understand the details of Arabidopsis BRI1 and BAK1 transphosphorylation and substrate phosphorylation (Wang et al., 2008). Similarly, we tested the ability of SlBRI1 to phosphorylate eight of these previously characterized peptide substrates.

Interestingly, SlBRI1 transphosphorylated synthetic peptides and was generally similar to Arabidopsis BRI1 in specificity. However, SlBRI1 was less discriminating with respect to the nature of the basic residues at the P−3 and P−4 positions. With Arabidopsis BRI1, there was a stronger preference for Lys over Arg and His (Oh et al., 2000) compared with SlBRI1 (this study). Accordingly, Arabidopsis BRI1 prefers the BR13 peptide (with Lys at P−3 and P−4) over the SP11 peptide (with Arg at both positions) and strongly disfavors the BR14 peptide with His at these two positions.

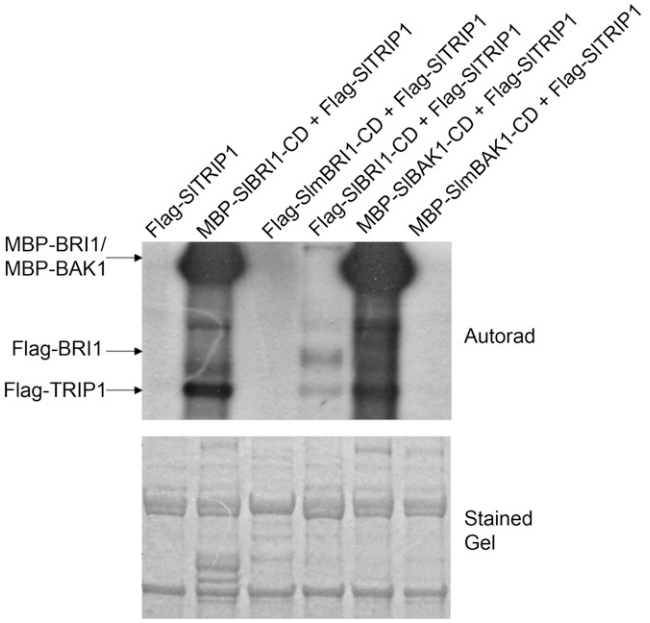

Figure 5. Both tomato BRI1-CD and BAK1-CD can phosphorylate Flag-SlTRIP1 in vitro. Assays containing 1 μg each of affinity-purified recombinant BRI1 or BAK1 cytoplasmic domains (the wild type or kinase-inactive mutants) and 5 μg of affinity-purified Flag-SlTRIP1 were incubated with 20 μCi of [γ-^{32}P]ATP in kinase buffer for 1 h, followed by 10% (w/v) SDS-PAGE and autoradiography.

In contrast, SlBRI1 does not display as dramatic a preference for BR13 over SP11, either in assays at fixed peptide concentrations (Fig. 1B) or when selectivity is assessed as the ratio of V_{max} to K_m (Fig. 2). Also, SlBRI1 had higher relative activity with the BR14 peptide, with His at P−3 and P−4, compared with Arabidopsis BRI1 (0.4 versus 0.2, respectively). Although not directly tested with SlBRI1, previous studies with Arabidopsis BRI1 indicated that basic residues at P−3 and P−4 were almost essential for transphosphorylation activity (Oh et al., 2000). It is likely that tomato BRI1 is similar but simply less discriminating in terms of the nature of the basic residue at these positions. Moreover, it is also worth noting that SlBAK1 had activity with the SP11 peptide that was significant and generally equivalent to SlBRI1 (Fig. 1C). This is in contrast to Arabidopsis BAK1, which has little or no activity with these synthetic peptides in vitro (Wang et al., 2008). Although tomato BAK1 was not further characterized in terms of peptide preferences, the differences between tomato and Arabidopsis BRI1 and BAK1 highlight the importance of studies from different species.

Another important similarity with Arabidopsis is that the combination of SlBRI1 with SlBAK1 resulted in reciprocal transphosphorylation of each of the partner kinases, assessed using kinase-inactive site-directed mutants of either SlBRI1 or SlBAK1 (Fig. 1A). We previously expressed different combinations of kinase-inactive and wild-type tagged versions of Arabidopsis BRI1 and BAK1 in the same transgenic plant and found that an active BRI1 kinase, but not BAK1 kinase, was required for BR-dependent association of the pair. Moreover, when BAK1-GFP was expressed in the *bri1-1* null mutant background, phosphorylation levels were dramatically reduced in BAK1-GFP (Wang et al., 2005, 2008). A range of in vitro kinase assays also showed that BAK1 stimulates BRI1 activity and that both BRI1 and BAK1 can transphosphorylate each other on specific residues. Based on these findings, we proposed a sequential transphosphorylation mechanism of BR signaling in which ligand-activated BRI1 heterodimerizes with BAK1, leading to BAK1 kinase activation by BRI1-mediated transphosphorylation of BAK1 activation loop residues, including the critical Thr-455 residue. The activated BAK1 in turn transphosphorylates BRI1 on juxtamembrane and C-terminal residues, increasing BR signaling by enhancing the phosphorylation of specific BRI1 substrates (Wang et al., 2008). In tomato, we have now shown that SlBRI1 transphosphorylates SlBAK1 on Thr-459, the residue equivalent to Thr-455 in Arabidopsis BAK1 (Table I). Furthermore, the end result of the transphosphorylation between active forms of both tomato kinases is enhanced SP11 peptide phosphorylation activity (Fig. 1C). However, unlike the situation with Arabidopsis BRI1 and BAK1, it cannot be concluded that the transphosphorylation activity of SlBRI1 was specifically increased by SlBAK1 transphosphorylation, as enhanced SlBAK1 activity directed against the SP11 peptide itself could also be involved. Further studies will be required to resolve this important point and to determine the extent to which the sequential transphosphorylation model applies to tomato BR signaling.

We previously examined the functional significance of each identified and predicted phosphorylation site in Arabidopsis BRI1 by site-directed mutagenesis of specific Ser, Thr, or Tyr residues followed by biochemical analysis in vitro and testing for the ability of the altered construct to rescue the weak *bri1-5* BR-insensitive mutant in planta. For biochemical function, we assessed the effect of mutagenesis on autophosphorylation of the BRI1 cytoplasmic domain in vitro and on phosphorylation of the BR13 synthetic peptide (Wang et al., 2005; Oh et al., 2009b). A similar analysis was conducted with tomato BRI1 to determine the functional significance of identified phosphorylation sites and their role in the biochemical function of SlBRI1. The juxtamembrane phosphorylation site Thr-872 appears to serve a negative regulatory role in Arabidopsis BRI1, as the T872A site-directed mutant has 10-fold higher activity against the BR13 peptide substrate compared with wild-type BRI1. The corresponding residue in tomato BRI1, Thr-877, is also phosphorylated, and the T877A site-directed mutant showed 20-fold higher activity with the BR13 peptide compared with the wild-type kinase. In contrast, Arabidopsis BRI1 juxtamembrane mutants Y831F, T842A, and S858A all showed substantially reduced peptide substrate phosphorylation (Wang et al., 2005; Oh et al., 2009b), while the corresponding tomato BRI1 residues showed increased (Y839F and T848A) or similar (S863A) peptide phosphorylation (Fig. 3B). Thus, there appears to be both conservation and divergence in the functional role of juxtamembrane phosphorylation between tomato and Arabidopsis BRI1, at least in vitro.

The activation of many protein kinases occurs by autophosphorylation of one to three residues within the activation loop of subdomain VII/VIII, which is thought to allow substrate access to the catalytic site in subdomain VIb (Johnson et al., 1996). We previously confirmed that both Arabidopsis BRI1 and BAK1 autophosphorylate on at least three residues within the activation loop in vivo and thus may share this activation mechanism with many animal kinases (Wang et al., 2005, 2008). Moreover, sequence alignment of plant RLKs reveals that the activation loop is highly conserved, including several Ser and Thr residues that are routinely present. In fact, the activation loop residue corresponding to Thr-1049 in Arabidopsis BRI1 and Thr-455 in BAK1 is nearly invariant in 100 of the most closely related Arabidopsis RLKs. This conserved residue is also present in tomato BRI1 (Thr-1054) and BAK1 (Thr-459), and we show here that this residue is phosphorylated in vitro in both tomato BRI1 and BAK1. Furthermore, functional analysis shows that tomato BRI1 Thr-1054 is essential for both autophosphorylation and peptide substrate phosphorylation in vitro (Fig. 3) and for normal BRI1 signaling and plant development in vivo (Fig. 4), as was previously demonstrated for

Arabidopsis residue Thr-1049 (Wang et al., 2005). However, the function of other BRI1 activation loop residues appears to differ between Arabidopsis and tomato. Tomato BRI1 site-directed mutant T1047A shows complete loss of kinase activity for both autophosphorylation and peptide substrate phosphorylation (Fig. 3), while the corresponding Arabidopsis BRI1 mutant, T1042A, exhibits substantial autophosphorylation activity and limited peptide substrate phosphorylation (Wang et al., 2005). Thus, as with juxtamembrane residues, there appears to be both conservation and divergence in the functional role of activation loop residue phosphorylation when comparing tomato and Arabidopsis BRI1.

Characterizing BR-dependent phosphorylation sites in cytoplasmic targets of BRI1 is essential for a complete understanding of BR action. In mammals, the TGF-β family of polypeptides are perceived at the cell surface by a complex of type I (RI) and type II (RII) TGF-β receptor Ser/Thr kinases. Mammalian TRIP1 binds to the cytoplasmic domain of the TGF-β RII receptor, is phosphorylated on Ser and Thr residues by the receptor kinase, and functions as a modulator of TGF-β receptor signaling in vivo (Choy and Derynck, 1998). Subsequently, TRIP1 was also shown to function as eIF3i in mammals (Asano et al., 1997), wheat (*Triticum aestivum*), and Arabidopsis (Burks et al., 2001). We previously found that the majority of Arabidopsis TRIP1 antisense and overexpression lines exhibited strong developmental phenotypes (Jiang and Clouse, 2001), that TRIP1 and BRI1 interact directly in planta, and that the BRI1 kinase domain phosphorylates Arabidopsis TRIP1 in vitro on at least three specific residues (Ehsan et al., 2005). These findings support a possible role for TRIP1 in the molecular mechanisms of BR-regulated growth and development in Arabidopsis. Here, we show that tomato BRI1 can also phosphorylate tomato TRIP1 on specific residues in vitro. Demonstration that BRI1 and TRIP1 also interact in planta will be necessary to show a functional role for the BRI1-TRIP1 interaction in tomato. Interestingly, the Tomato Expression Database (http://ted.bti.cornell.edu) shows that TRIP1 (represented by probes 1-1-6.4.20.15 and 1-1-7.4.13.21 on the TOM1 microarray) is expressed in immature fruit. Furthermore, genes encoding BR biosynthetic enzymes are expressed, endogenous BRs accumulate to significant levels in developing tomato fruit during the cell expansion phase (Montoya et al., 2005), and application of exogenous BRs promotes tomato fruit ripening (Vidya Vardhini and Rao, 2002). Therefore, SlBRI1-mediated BR signaling is likely to be active during the same period when TRIP1 is showing increased expression in developing tomato fruit, suggesting that studies of the interaction and phosphorylation of SlBRI1 and SlTRIP1 at various stages of tomato fruit development might be a productive avenue of future experiments that would not be possible in Arabidopsis.

In summary, we have identified several specific sites of phosphorylation in both tomato BRI1 and BAK1 receptor kinases and have initiated a functional characterization of selected BRI1 sites and their role in kinase function and BR signaling. This work provides a foundation for future characterization of additional sites in vivo and their role in regulating BR signaling pathways involved in vegetative and reproductive development in tomato, an important horticultural crop.

MATERIALS AND METHODS

Cloning SlBRI1 and SlBAK1 Cytoplasmic Domains and SlTRIP1 for Bacterial Expression

The tomato (*Solanum lycopersicum*) BRI1 cytoplasmic domain was amplified from tomato genomic DNA with sense (5′-CGATCTCGAGGAGACGAAGAAGAGGAGGAGG-3′) and antisense (5′-CGATGGTACCTCAAAGGTGTTTGCTCAGCTC-3′) primers. The purified PCR product was digested with *Xho*I/*Kpn*I (New England Biolabs), gel purified, and ligated with *Xho*I/*Kpn*I-digested, gel-purified pFlag-MAC (Sigma) expression vector to yield Flag-SlBRI-CD, containing an N-terminal Flag epitope tag (DYKDDDDKVKL) followed by amino acids 824 through 1,207 of SlBRI1. The construct was completely sequenced to verify 100% identity with the SlBRI1 genomic sequence. Transformation of Flag-SlBRI-CD into pG-Tf2/BL21 *Escherichia coli* cells containing GroES-GroEL-tig chaperones was performed as described in the manufacturer's instructions (Takara Bio). A second *E. coli* expression construct, MBP-SlBRI1, was generated in pMAL-c4X expression vector (New England Biolabs) using the procedures described above. To generate a kinase-inactive mutant, Flag-SlBRI1(K916E), the conserved Lys at position 916 in subdomain II was substituted with Glu, using the QuickChange site-directed mutagenesis kit (Stratagene) with sense (5′-GAGTGTTGTAGCTATTGAGAAATTGATACACG-3′) and antisense (5′-CGTGTATCAATTTCTCAATAGCTACAACACTC-3′) primers. The resulting construct was sequenced to verify the correct mutation.

The SlBAK1 cytoplasmic domain was amplified by PCR from cDNA of tomato cv Heinz 5-d-old seedlings using primers MALBAK1CD_F3 (5′-AGGAATTCCGTCGAAAACCGGAAGACCAC-3′) + MALBAK1CD_R2 (5′-ATAAGCTTTCATCTTGGCCCTGATAACTCATC-3′). The BAK1 kinase-inactive mutation (K321E) was generated by PCR-induced mutagenesis using the following primer pairs, MALBAK1CD_F3 + mBAK1CD_R (5′-CCTCTTTTAATCTTTCAACAGCAACTAAAGAG-3′) and mBAK1CD_F (5′-TAGTTGCTGTTGAAAGATTAAAAGAGGAGC-3′) + MALBAK1CD_R2, to produce two PCR products. The two PCR products were pooled, and primers MALBAK1CD_F3 + MALBAK1CD_R2 were used to generate mutant BAK1-CD. Both wild-type and mutant BAK1CD were cloned into pGemT-easy (Promega) and sequenced. Wild-type and mutant *BAK1-CD* were digested from pGemT-easy with *Hin*dIII and *Eco*RI and were cloned into pMALC2E (New England Biolabs) to form N-terminal fusions with the MBP tag. Clones were sequenced to confirm MBP fusions.

SlTRIP1 was amplified by PCR from cDNA of tomato cv Cobra seedlings using forward primer 5′-CGATAAGCTTAGGCCAATATTGATGAAGGGCC-3′ and reverse primer 5′-GACTCTCGAGCTAAATCCTGATGTTGAAGTAATCC-3′. The gel-purified PCR product was digested with *Hin*dIII/*Xho*I (Promega), gel purified, and ligated with *Hin*dIII/*Xho*I-digested, gel-purified pFlag-MAC (Sigma) to obtain Flag-SlTRIP1. The construct was confirmed by DNA sequencing. The Flag-SlBRI-CD construct was transformed into *E. coli* BL21 (DE3) cells (Stratagene).

Purification and Biochemical Analysis of Recombinant Proteins

The purification of Flag-tagged fusion constructs with M2 agarose beads was conducted essentially as per the manufacturer's instructions (Sigma-Aldrich), using Flag peptide (20 mM Tris-HCl, pH 7.4, 200 mM NaCl, 1 mM EDTA, and 0.25 mg mL^{-1} Flag peptide) to elute Flag-SlBRI1-CD from the agarose beads. Purification of the MBP-tagged proteins using amylose resin was carried out per the manufacturer's instructions (New England Biolabs) except that the concentration of maltose in the elution buffer was 20 mM rather than 10 mM.

For autophosphorylation assays, a 40-μL reaction containing 1 μg of affinity-purified Flag-SlBRI1-CD, MBP-SlBRI1-CD, or MBP-SlBAK1-CD was incubated with 20 μCi of [γ-^{32}P]ATP in kinase buffer (50 mM HEPES-KOH, pH

7.9, 10 mM $MnCl_2$, 1.0 mM dithiothreitol, and 0.2 mM unlabeled ATP) at room temperature for 1 h. Reactions were terminated by adding 20 μL of 2× Laemmli loading buffer (Laemmli, 1970), heating the sample at 95°C for 5 min, followed by 10% (w/v) SDS-PAGE and autoradiography. Peptide substrate assays were performed as described (Oh et al., 2000) with some changes in protein and peptide amounts. A 20-μL reaction contained 0.10 mg mL^{-1} synthetic peptide, 0.5 μg of Flag-SlBRI1-CD, MBP-SlBRI1-CD, or MBP-SlBAK1-CD, 0.8 μCi of [γ-^{32}P]ATP, and 0.1 mM unlabeled ATP in a kinase buffer consisting of 50 mM MOPS, pH 7.4, 10 mM $MgCl_2$, and 0.2 mM $CaCl_2$. Each reaction point was determined in triplicate, and the results are presented as means ± SE.

For functional analysis of phosphorylation sites, the Flag-SlBRI1-CD construct was used as the template for site-directed mutagenesis of specific Ser, Thr, and Tyr residues using the QuickChange II site-directed mutagenesis kit (Stratagene). Fourteen in vitro mutant constructs containing substitutions in the SlBRI1 amino acid residues, T825A, Y839F, S846A, T848A, S863A, T877A, S968A, S1040A, T1044A, T1047A, S1049A, T1050A, T1054A, and S1073A, were generated. All constructs were sequenced completely to verify the presence of correct mutations and the absence of other unexpected mutations. Recombinant proteins containing specific mutations were analyzed by autophosphorylation and peptide substrate phosphorylation as described above.

Determination of in Vitro Autophosphorylation and Transphosphorylation Sites of SlBRI1 and SlBAK1 by Q-TOF LC-MS/MS and Q-TOF LC/MS^E Analysis

Five micrograms of affinity-purified recombinant proteins (Flag-SlBRI1-CD, MBP-SlBRI1-CD, and MBP-SlBAK1-CD) was autophosphorylated in kinase buffer (50 mM HEPES-KOH, pH 7.9, 10 mM $MnCl_2$, 1.0 mM dithiothreitol, and 0.2 mM unlabeled ATP) and separated on a 10% Bis-Tris Nu-PAGE gel (Invitrogen). The protein bands were excised, and in-gel reduction, alkylation, and trypsin digestion were performed on the excised bands according to a published protocol (Rowley et al., 2000). After digestion, peptides were extracted in 5% (v/v) formic acid, 50% (v/v) acetonitrile, and 45% (v/v) 50 mM NH_4HCO_3. Aliquots of digested peptides were also enriched for phosphopeptides using PHOS-select iron affinity gels (Sigma) according to the manufacturer's instructions. The peptide samples were then filtered and injected into a nanoACQUITY ultra-performance liquid chromatograph coupled to a Q-TOF Premier mass spectrometer (Waters) equipped with a NanoLockSpray ion source (Waters). The injected peptides were first desalted and concentrated on a 300-μm × 1-cm C18 trapping column at a flow rate of 10 μL min^{-1}. The trapped peptides were then separated by an in-line 25-cm × 75-μm (Waters) C18 column packed with Bridged Ethyl Hybrid C18 matrix (Waters) as the stationary phase and using a mobile phase linear gradient composed of 0.1% formic acid in water (A) and 0.1% formic acid in acetonitrile (B), from 7% B to 40% B over 60 min at flow rate of 300 nL min^{-1}.

The peptide samples were analyzed using data-dependent acquisition LC-MS/MS and data-independent acquisition LC/MS^E modes. In data-dependent acquisition mode, the top eight most intense ions were selected in each survey scan and were subjected to collision-induced dissociation to obtain product ion spectra. In the LC/MS^E mode, data were obtained by capturing alternating scans of 2 s each between low (4 V) and high (10–32 V) collision energies (Blackburn et al., 2010), where the low-energy scans generated intact peptide precursor ions and high-energy scans resulted in peptide product ions, resulting in better overall coverage from low- to high-intensity ions. A predigested standard, rabbit phosphorylase B, was analyzed periodically between samples to verify instrument sensitivity and performance. The raw data files obtained from LC-MS/MS analyses were searched against an *E. coli* database with the addition of tomato Flag-SlBRI1-CD, MBP-SlBRI1-CD, and MBP-SlBAK1-CD protein sequences using the Mascot 2.2 search algorithm (Matrix Science) running on an in-house server. The raw data obtained from LC/MS^E analyses were processed using ProteinLynx Global Server 2.4 software (Waters). Both LC-MS/MS and LC/MS^E data sets were searched with a fixed carbamidomethyl modification for Cys residues, along with variable modifications for Met oxidation, Asn and Gln deamidation, N-terminal acetylation, and phosphorylation of Ser, Thr, and Tyr residues.

Cloning of *SlBRI1-Flag* into Plant Transformation Vectors

SlBRI1 was PCR amplified from tomato genomic DNA with sense (5′-CGATCCCGGGAGTTTTTATTTTTAATTTTCTTTCAAATACTTCCATCATGAAAGCTCACAAAACTGTG-3′) and antisense (5′-GACTGAGCTCTCATTTGTCATCGTCGTCCTTGTAGTCAAGGTGTTTGCTCAGCTCCATTG-3′) primers. The sense primer contained a 37-bp untranslated region sequence from *Alfalfa mosaic virus* upstream of the SlBRI1 start sequence that has been shown previously to enhance the expression of transgenes in transformed tomato plants (Krasnyanski et al., 2001). The PCR product was gel purified, digested with *Sma*I and *Sac*I, and introduced into the binary vector pBI121 (Clontech) that had also been digested with *Sma*I/*Sac*I and gel purified to remove the *uidA* gene, to yield the plasmid (35S:SlBRI1-Flag/pBI121).

To obtain full-length SlBRI1 with the T1054A mutation, the first 2,484 bp of SlBRI1 was PCR amplified from 35S:SlBRI1-Flag/pBI121 using the sense primer 5′-CGATCCCGGGAGTTTTTATTTTTAATTTTCTTTCAAATACTTCCATCATGAAAGCTCACAAAACTGTG-3′ and antisense primer 5′-GACTGAGCTCAGTCAGGCCTCTTCTTCGTCTCTATGG-3′. The resulting PCR product was gel purified and cloned into the pGemT-easy Vector (Promega). The *SlBRI1-CD* gene carrying the T1054A mutation was amplified from the mutant Flag-SlBRI1-CD construct using the PCR primer pair 5′-AGGAGGAAGAAGGAGGCTGC-3′ (forward) and 5′-GACTGAGCTCTCATTTGTCATCGTCGTCCTTGTAGTCAAGGTGTTTGCTCAGCTCCATTG-3′ (reverse). To obtain the full-length mutant SlBRI1-Flag construct in the pGemT-easy vector, the amplified PCR product was gel purified, digested with *Stu*I/*Sac*I (Promega), gel purified, and ligated with a *Stu*I/*Sac*I digested, gel purified pGemT-easy vector containing the first 2,484 bp of SlBRI1. All constructs were sequenced completely.

The *Eco*RI/*Hin*dIII *nosp-uidA* segment of pGPTV-KAN (Becker et al., 1992) was replaced with 35S-GUS containing the *Eco*RI/*Hin*dIII fragment of the plasmid pBI121 to obtain pGPTV-35S-KAN. Full-length *SlBRI1-Flag-T1054A* was released from pGemT-easy using *Sma*I/*Sac*I restriction enzymes, gel purified, and ligated into *Sma*I/*Sac*I-digested, gel purified pGPTV-35S-KAN. The wild-type SlBRI1-Flag construct was transferred from 35S:SlBRI1-Flag/pBI121 into pGPTV-35S-KAN by *Sma*I/*Sac*I digestion and ligation.

Transformation of the Tomato *cu3^{-abs}* Mutant with *SlBRI1-Flag* Constructs

Agrobacterium tumefaciens-mediated transformation was performed essentially as described by Krasnyanski et al. (2001) with modifications. Seeds of the weak allele of SlBRI1, *cu3^{-abs}* (Montoya et al., 2002), were sterilized with 70% ethanol for 1 min and 50% Clorox for 30 min. After sterilization, seeds were rinsed four times with sterile water and germinated on tomato seedling medium (1× Murashige and Skoog [MS] salts + Gamborg's B5 vitamins, 10 g L^{-1} Suc, and 12 g L^{-1} agar, pH 5.6) in glass jars. Eight-day-old seedlings grown under 16 h of light and 8 h of dark at 25°C were used for cotyledon explants.

A. tumefaciens strain GV3101 containing SlBRI1-Flag/pGPTV-35S-KAN plasmids was cultured in 25 mL of liquid YEP medium (10 g L^{-1} yeast extract [Bacto], 10 g L^{-1} Bacto-peptone, and 5 g L^{-1} NaCl) containing 100 mg L^{-1} kanamycin, 50 mg L^{-1} rifampicin, and 50 mg L^{-1} gentamycin and grown overnight on a shaker at 220 rpm at 28°C. The overnight *A. tumefaciens* culture was centrifuged at 1,000*g* for 30 min to precipitate the cells. The cell pellet was resuspended in 25 mL of liquid resuspension (LR) medium (1× MS salts + MS vitamins, 30 g L^{-1} Suc, 2.0 g L^{-1} Glc, and 700 mg L^{-1} MES, pH 6.0) with 40 mg L^{-1} acetosyringone and grown for another 1 to 2 h at 28°C. The suspension was then diluted to an optical density at 600 nm of 0.3 to 0.4 with LR medium containing 40 mg L^{-1} acetosyringone. Cotyledon explants were placed on petri plates containing tomato cocultivation medium (1× MS salts + MS vitamins, 30 g L^{-1} Suc, 2.0 g L^{-1} Glc, 0.5 mg L^{-1} naphthylacetic acid, 1.0 mg L^{-1} benzyladenine, 700 mg L^{-1} MES, 40 mg L^{-1} acetosyringone, and 12 g L^{-1} agar, pH 5.6) and wounded with multipronged needles. Wounded cotyledons were submerged in diluted liquid *A. tumefaciens* suspension for 15 min with shaking at 50 rpm. Following inoculation, cotyledons were blotted dry on sterile paper towels and placed back on tomato cocultivation medium for 48 h in the dark at 25°C.

After cocultivation, explants were washed two to three times with LR medium containing 300 mg L^{-1} timentin, blotted dry on sterile paper towels, and placed (15–20 explants per plate) on tomato shoot regeneration (TSR) medium (1× MS salts + MS vitamins, 30 g L^{-1} Suc, 0.1 mg L^{-1} indole-3-acetic acid, 2.0 mg L^{-1} zeatin, 300 mg L^{-1} timentin, 100 mg L^{-1} kanamycin, 40 mg L^{-1} acetosyringone, and 8.0 g L^{-1} agar, pH 5.6). After 2 weeks on TSR medium, the explants were subcultured onto fresh TSR medium and further cultured under a 16-h photoperiod (provided by 20-W cool-white fluorescent tubes yielding a light intensity of 30 mmol m^{-2} s^{-1}) at 25°C. Five to 6 weeks later, 1- to 2-cm-long shoots were excised and placed on a tomato rooting medium (1× MS salts + MS vitamins, 30 g L^{-1} Suc, 300 mg L^{-1} timentin, 100 mg L^{-1} kanamycin, and 8.0 g L^{-1} agar, pH 5.6) for secondary selection. Tomato plants with well-developed roots were transferred into small plastic pots with sterile soil and covered with clear

plastic covers for 1 week of acclimatization in a growth chamber. Following acclimatization, plants were transferred to the greenhouse for further growth.

PCR to Monitor SlBRI1-Flag Transgene Expression

Total RNA was isolated from 300 mg of leaves harvested from transgenic tomato plants of identical age followed by grinding in liquid nitrogen$_2$ and isolation of RNA using the RNeasy kit (Qiagen). Two micrograms of total RNA was used for the synthesis of first-strand cDNA with the RETROscript reverse transcription system using oligo(dT) primer (Ambion). PCR amplification of cDNA used the following primers: 5′-ATGACTCAAATCATGTTTGAGACC-3′ and 5′-GATCTTCATGCTGCTTGGAGC-3′ for actin; 5′-GAAGCCAGAGTATCTGATTTC-3′ and 5′-CTCATACACTATTATATACAACACTG-3′ for endogenous SlBRI1; and 5′-GAAGCCAGAGTATCTGATTTC-3′ and 5′-ACTTGTCATCGTCATCCTTG-3′ for transgenic SlBRI1-Flag. PCR was performed for 35 cycles of 94°C for 15 s, 55°C for 1.5 min, and 72°C for 1.5 min, followed by a single extension of 10 min at 72°C.

Supplemental Data

The following materials are available in the online version of this article.

Supplemental Figure S1. BRI1 phosphorylation product ion spectra.

Supplemental Figure S2. BAK1 phosphorylation product ion spectra.

Supplemental Figure S3. BAK1 transphosphorylation product ion spectrum.

Supplemental Figure S4. TRIP1 transphosphorylation product ion spectrum.

Received May 16, 2013; accepted July 1, 2013; published July 10, 2013.

LITERATURE CITED

Asano K, Kinzy TG, Merrick WC, Hershey JW (1997) Conservation and diversity of eukaryotic translation initiation factor eIF3. J Biol Chem **272:** 1101–1109

Becker D, Kemper E, Schell J, Masterson R (1992) New plant binary vectors with selectable markers located proximal to the left T-DNA border. Plant Mol Biol **20:** 1195–1197

Bishop GJ, Nomura T, Yokota T, Harrison K, Noguchi T, Fujioka S, Takatsuto S, Jones JD, Kamiya Y (1999) The tomato DWARF enzyme catalyses C-6 oxidation in brassinosteroid biosynthesis. Proc Natl Acad Sci USA **96:** 1761–1766

Blackburn K, Cheng FY, Williamson JD, Goshe MB (2010) Data-independent liquid chromatography/mass spectrometry (LC/MS(E)) detection and quantification of the secreted *Apium graveolens* pathogen defense protein mannitol dehydrogenase. Rapid Commun Mass Spectrom **24:** 1009–1016

Burks EA, Bezerra PP, Le H, Gallie DR, Browning KS (2001) Plant initiation factor 3 subunit composition resembles mammalian initiation factor 3 and has a novel subunit. J Biol Chem **276:** 2122–2131

Chono M, Honda I, Zeniya H, Yoneyama K, Saisho D, Takeda K, Takatsuto S, Hoshino T, Watanabe Y (2003) A semidwarf phenotype of barley uzu results from a nucleotide substitution in the gene encoding a putative brassinosteroid receptor. Plant Physiol **133:** 1209–1219

Choy L, Derynck R (1998) The type II transforming growth factor (TGF)-beta receptor-interacting protein TRIP-1 acts as a modulator of the TGF-beta response. J Biol Chem **273:** 31455–31462

Clouse SD (2011a) Brassinosteroid signal transduction: from receptor kinase activation to transcriptional networks regulating plant development. Plant Cell **23:** 1219–1230

Clouse SD (2011b) Brassinosteroids. The Arabidopsis Book **9:** e0151. doi: 10.1199/tab.0151

Clouse SD, Langford M, McMorris TC (1996) A brassinosteroid-insensitive mutant in *Arabidopsis thaliana* exhibits multiple defects in growth and development. Plant Physiol **111:** 671–678

Ehsan H, Ray WK, Phinney B, Wang X, Huber SC, Clouse SD (2005) Interaction of Arabidopsis BRASSINOSTEROID-INSENSITIVE 1 receptor kinase with a homolog of mammalian TGF-beta receptor interacting protein. Plant J **43:** 251–261

Friedrichsen DM, Joazeiro CA, Li J, Hunter T, Chory J (2000) Brassinosteroid-insensitive-1 is a ubiquitously expressed leucine-rich repeat receptor serine/threonine kinase. Plant Physiol **123:** 1247–1256

He JX, Gendron JM, Sun Y, Gampala SS, Gendron N, Sun CQ, Wang ZY (2005) BZR1 is a transcriptional repressor with dual roles in brassinosteroid homeostasis and growth responses. Science **307:** 1634–1638

Holton N, Caño-Delgado A, Harrison K, Montoya T, Chory J, Bishop GJ (2007) Tomato BRASSINOSTEROID INSENSITIVE1 is required for systemin-induced root elongation in *Solanum pimpinellifolium* but is not essential for wound signaling. Plant Cell **19:** 1709–1717

Hothorn M, Belkhadir Y, Dreux M, Dabi T, Noel JP, Wilson IA, Chory J (2011) Structural basis of steroid hormone perception by the receptor kinase BRI1. Nature **474:** 467–471

Jiang J, Clouse SD (2001) Expression of a plant gene with sequence similarity to animal TGF-beta receptor interacting protein is regulated by brassinosteroids and required for normal plant development. Plant J **26:** 35–45

Johnson LN, Noble ME, Owen DJ (1996) Active and inactive protein kinases: structural basis for regulation. Cell **85:** 149–158

Karlova R, Boeren S, van Dongen W, Kwaaitaal M, Aker J, Vervoort J, de Vries S (2009) Identification of *in vitro* phosphorylation sites in the *Arabidopsis thaliana* somatic embryogenesis receptor-like kinases. Proteomics **9:** 368–379

Kauschmann A, Jessop A, Koncz C, Szekeres M, Willmitzer L, Altmann T (1996) Genetic evidence for an essential role of brassinosteroids in plant development. Plant J **9:** 701–713

Kim TW, Guan S, Sun Y, Deng Z, Tang W, Shang JX, Sun Y, Burlingame AL, Wang ZY (2009) Brassinosteroid signal transduction from cell-surface receptor kinases to nuclear transcription factors. Nat Cell Biol **11:** 1254–1260

Kim TW, Wang ZY (2010) Brassinosteroid signal transduction from receptor kinases to transcription factors. Annu Rev Plant Biol **61:** 681–704

Koka CV, Cerny RE, Gardner RG, Noguchi T, Fujioka S, Takatsuto S, Yoshida S, Clouse SD (2000) A putative role for the tomato genes *DUMPY* and *CURL-3* in brassinosteroid biosynthesis and response. Plant Physiol **122:** 85–98

Krasnyanski S, Sandhu J, Domier L, Buetow D, Korban S (2001) Effect of an enhanced CaMV 35S promoter and a fruit-specific promoter on uida gene expression in transgenic tomato plants. In Vitro Cell Dev Biol Plant **37:** 427–433

Laemmli UK (1970) Cleavage of structural proteins during the assembly of the head of bacteriophage T4. Nature **227:** 680–685

Li J, Chory J (1997) A putative leucine-rich repeat receptor kinase involved in brassinosteroid signal transduction. Cell **90:** 929–938

Li J, Wen J, Lease KA, Doke JT, Tax FE, Walker JC (2002) BAK1, an Arabidopsis LRR receptor-like protein kinase, interacts with BRI1 and modulates brassinosteroid signaling. Cell **110:** 213–222

Mantelin S, Peng HC, Li B, Atamian HS, Takken FL, Kaloshian I (2011) The receptor-like kinase SlSERK1 is required for Mi-1-mediated resistance to potato aphids in tomato. Plant J **67:** 459–471

Montoya T, Nomura T, Farrar K, Kaneta T, Yokota T, Bishop GJ (2002) Cloning the tomato *curl3* gene highlights the putative dual role of the leucine-rich repeat receptor kinase tBRI1/SR160 in plant steroid hormone and peptide hormone signaling. Plant Cell **14:** 3163–3176

Montoya T, Nomura T, Yokota T, Farrar K, Harrison K, Jones JDG, Kaneta T, Kamiya Y, Szekeres M, Bishop GJ (2005) Patterns of Dwarf expression and brassinosteroid accumulation in tomato reveal the importance of brassinosteroid synthesis during fruit development. Plant J **42:** 262–269

Morinaka Y, Sakamoto T, Inukai Y, Agetsuma M, Kitano H, Ashikari M, Matsuoka M (2006) Morphological alteration caused by brassinosteroid insensitivity increases the biomass and grain production of rice. Plant Physiol **141:** 924–931

Nam KH, Li J (2002) BRI1/BAK1, a receptor kinase pair mediating brassinosteroid signaling. Cell **110:** 203–212

Noguchi T, Fujioka S, Choe S, Takatsuto S, Yoshida S, Yuan H, Feldmann KA, Tax FE (1999) Brassinosteroid-insensitive dwarf mutants of Arabidopsis accumulate brassinosteroids. Plant Physiol **121:** 743–752

Nomura T, Bishop GJ, Kaneta T, Reid JB, Chory J, Yokota T (2003) The LKA gene is a BRASSINOSTEROID INSENSITIVE 1 homolog of pea. Plant J **36:** 291–300

Nomura T, Nakayama M, Reid JB, Takeuchi Y, Yokota T (1997) Blockage of brassinosteroid biosynthesis and sensitivity causes dwarfism in garden pea. Plant Physiol **113:** 31–37

Oh MH, Clouse SD, Huber SC (2009a) Tyrosine phosphorylation in brassinosteroid signaling. Plant Signal Behav **4:** 1182–1185

Oh MH, Ray WK, Huber SC, Asara JM, Gage DA, Clouse SD (2000) Recombinant brassinosteroid insensitive 1 receptor-like kinase autophosphorylates

on serine and threonine residues and phosphorylates a conserved peptide motif in vitro. Plant Physiol **124:** 751–766

Oh MH, Sun J, Oh DH, Zielinski RE, Clouse SD, Huber SC (2011) Enhancing Arabidopsis leaf growth by engineering the BRASSINOSTEROID INSENSITIVE1 receptor kinase. Plant Physiol **157:** 120–131

Oh MH, Wang X, Kota U, Goshe MB, Clouse SD, Huber SC (2009b) Tyrosine phosphorylation of the BRI1 receptor kinase emerges as a component of brassinosteroid signaling in Arabidopsis. Proc Natl Acad Sci USA **106:** 658–663

Oh MH, Wang X, Wu X, Zhao Y, Clouse SD, Huber SC (2010) Autophosphorylation of Tyr-610 in the receptor kinase BAK1 plays a role in brassinosteroid signaling and basal defense gene expression. Proc Natl Acad Sci USA **107:** 17827–17832

Rowley A, Choudhary JS, Marzioch M, Ward MA, Weir M, Solari RC, Blackstock WP (2000) Applications of protein mass spectrometry in cell biology. Methods **20:** 383–397

She J, Han Z, Kim TW, Wang J, Cheng W, Chang J, Shi S, Wang J, Yang M, Wang ZY, et al (2011) Structural insight into brassinosteroid perception by BRI1. Nature **474:** 472–476

Sun Y, Fan XY, Cao DM, Tang W, He K, Zhu JY, He JX, Bai MY, Zhu S, Oh E, et al (2010) Integration of brassinosteroid signal transduction with the transcription network for plant growth regulation in Arabidopsis. Dev Cell **19:** 765–777

Tang W, Yuan M, Wang R, Yang Y, Wang C, Oses-Prieto JA, Kim TW, Zhou HW, Deng Z, Gampala SS, et al (2011) PP2A activates brassinosteroid-responsive gene expression and plant growth by dephosphorylating BZR1. Nat Cell Biol **13:** 124–131

Vidya Vardhini B, Rao SS (2002) Acceleration of ripening of tomato pericarp discs by brassinosteroids. Phytochemistry **61:** 843–847

Wang X, Goshe MB, Soderblom EJ, Phinney BS, Kuchar JA, Li J, Asami T, Yoshida S, Huber SC, Clouse SD (2005) Identification and functional analysis of in vivo phosphorylation sites of the *Arabidopsis* BRASSINOSTEROID-INSENSITIVE1 receptor kinase. Plant Cell **17:** 1685–1703

Wang X, Kota U, He K, Blackburn K, Li J, Goshe MB, Huber SC, Clouse SD (2008) Sequential transphosphorylation of the BRI1/BAK1 receptor kinase complex impacts early events in brassinosteroid signaling. Dev Cell **15:** 220–235

Wang ZY, Bai MY, Oh E, Zhu JY (2012) Brassinosteroid signaling network and regulation of photomorphogenesis. Annu Rev Genet **46:** 701–724

Weekes J, Ball KL, Caudwell FB, Hardie DG (1993) Specificity determinants for the AMP-activated protein kinase and its plant homologue analysed using synthetic peptides. FEBS Lett **334:** 335–339

Yamamuro C, Ihara Y, Wu X, Noguchi T, Fujioka S, Takatsuto S, Ashikari M, Kitano H, Matsuoka M (2000) Loss of function of a rice *brassinosteroid insensitive1* homolog prevents internode elongation and bending of the lamina joint. Plant Cell **12:** 1591–1606

Yin Y, Vafeados D, Tao Y, Yoshida S, Asami T, Chory J (2005) A new class of transcription factors mediates brassinosteroid-regulated gene expression in Arabidopsis. Cell **120:** 249–259

Yu X, Li L, Zola J, Aluru M, Ye H, Foudree A, Guo H, Anderson S, Aluru S, Liu P, et al (2011) A brassinosteroid transcriptional network revealed by genome-wide identification of BESI target genes in *Arabidopsis thaliana*. Plant J **65:** 634–646